



Simulation of dual carbon–bromine stable isotope fractionation during 1,2-dibromoethane degradation

Jin, Biao; Nijenhuis, Ivonne; Rolle, Massimo

Published in:
Isotopes in Environmental and Health Studies

Link to article, DOI:
[10.1080/10256016.2018.1468759](https://doi.org/10.1080/10256016.2018.1468759)

Publication date:
2018

Document Version
Peer reviewed version

[Link back to DTU Orbit](#)

Citation (APA):
Jin, B., Nijenhuis, I., & Rolle, M. (2018). Simulation of dual carbon–bromine stable isotope fractionation during 1,2-dibromoethane degradation. *Isotopes in Environmental and Health Studies*, 54(4), 418-434.
<https://doi.org/10.1080/10256016.2018.1468759>

General rights

Copyright and moral rights for the publications made accessible in the public portal are retained by the authors and/or other copyright owners and it is a condition of accessing publications that users recognise and abide by the legal requirements associated with these rights.

- Users may download and print one copy of any publication from the public portal for the purpose of private study or research.
- You may not further distribute the material or use it for any profit-making activity or commercial gain
- You may freely distribute the URL identifying the publication in the public portal

If you believe that this document breaches copyright please contact us providing details, and we will remove access to the work immediately and investigate your claim.

This is a Post Print of the article published on line 1st June 2018 in Isotope in Environmental and Health Studies. The publishers' version is available at the permanent link: <https://doi.org/10.1080/10256016.2018.1468759>

Simulation of Dual Carbon–Bromine Stable Isotope Fractionation during 1,2-Dibromoethane Degradation

Biao Jin^{a,b*}, Ivonne Nijenhuis^c, Massimo Rolle^a

^a Department of Environmental Engineering, Technical University of Denmark, Miljøvej Building
113, DK-2800 Kgs. Lyngby, Denmark

^b State Key Laboratory of Organic Geochemistry, Guangzhou Institute of Geochemistry, Chinese
Academy of Sciences, Kehua Street 511, 510640 Guangzhou, China

^c Department of Isotope Biogeochemistry, Helmholtz-Centre for Environmental Research - UFZ,
Permoserstrasse 15, 04318 Leipzig, Germany

* Corresponding author phone: +45 45251566; e-mail: bjin@env.dtu.dk

27 **Abstract**

28 We performed a model-based investigation to simultaneously predict the evolution of concentration,
29 as well as stable carbon and bromine isotope fractionation during 1,2-dibromoethane (EDB,
30 ethylene dibromide) transformation in a closed system. The modelling approach considers bond-
31 cleavage mechanisms during different reactions and allows evaluating dual carbon-bromine isotopic
32 signals for chemical and biotic reactions, including aerobic and anaerobic biological transformation,
33 dibromoelimination by Zn(0) and alkaline hydrolysis. The proposed model allowed us to accurately
34 simulate the evolution of concentrations and isotope data observed in a previous laboratory study
35 and to successfully identify different reaction pathways. Furthermore, we illustrated the model
36 capabilities in degradation scenarios involving complex reaction systems. Specifically, we
37 examined (i) the case of sequential multistep transformation of EDB and the isotopic evolution of
38 the parent compound, the intermediate and the reaction product, and (ii) the case of parallel
39 competing abiotic pathways of EDB transformation in alkaline solution.

40

41 **Keywords:** degradation; organic contaminants; isotope modelling; compound-specific isotope
42 analysis; stable carbon and bromine isotopes

43

44

45

46 **1. Introduction**

47 In the last few decades, 1,2-dibromoethane (EDB, ethylene dibromide) has been frequently detected
48 in drinking water and natural aquatic systems, due to its extensive application as an agricultural
49 fumigant as well as a lead scavenger in gasoline [1,2]. EDB is a widespread pollutant and several
50 studies have investigated its degradation under different environmental conditions [3–5]. However,
51 the environmental fate of EDB is difficult to understand and to quantitatively assess since this
52 chemical can undergo different transformation processes and its concentration distribution in
53 aquatic systems also depends on physical processes such as mass-transfer, dilution and sorption [6–
54 8]. Therefore, the application of compound specific isotope analysis (CSIA) is beneficial to
55 investigate the environmental fate of EDB. CSIA techniques have been developed and applied to a
56 wide variety of organic pollutants [9–12], for which the determination of the change of stable
57 isotope signals could be used to identify and quantify specific transformation processes. Carbon is
58 the most common element for CSIA applications in contaminant hydrology; however, recent
59 developments on analytical techniques for chlorine and bromine CSIA allowed increasing
60 applications of dual-element isotope analysis for organohalides [13–18]. Thus, different reaction
61 pathways of halogenated organic pollutants could be characterized and understood using dual-
62 element CSIA [19–23]. In a very recent laboratory study, Kuntze et al. [24] applied dual carbon-
63 bromine CSIA to investigate different reaction mechanisms during EDB degradation.

64 In this work we propose an isotope modelling approach for dual carbon-bromine isotope
65 fractionation based on the reaction mechanisms and the experimental data from the study of Kuntze
66 et al. [24]. Isotope models are valuable tools to provide quantitative interpretation of isotopic data
67 obtained during different transformation processes as well as in complex environmental systems
68 where both physical and transformation processes influence the observed isotopic signals [25–27].
69 So far, isotope models have been developed and applied for multi-element isotopic prediction of

various organic contaminants, including chlorinated hydrocarbons [28–31], BTEX compounds [32,33] and organic pesticides [34,35]. However, such a modelling framework is still lacking for brominated organic compounds. This modelling case study illustrates an integrated carbon-bromine isotope modelling approach to simultaneously predict the evolution of concentration, as well as carbon and bromine isotopic signals. Our work focuses on chemical and biotic transformations of EDB with the specific goals to: (i) describe a mechanism-based integrated modelling approach to simulate carbon and bromine isotope fractionation; (ii) validate the model with the isotopic data observed during EDB degradation reactions; (iii) illustrate the capabilities of the model based on scenarios of complex EDB degradation pathways, including multistep reactions and parallel degradation pathways, and considering the evolution of dual C and Br isotope signals not only of EDB but also of its degradation intermediates and products.

81

2. Modelling approach

2.1. Degradation pathways and reaction mechanisms

We focus on EDB degradation through two important degradation pathways, dibromoelimination and nucleophilic substitution (S_N2). The two degradation pathways can occur both chemically and biotically. Dibromoelimination occurs during reduction of EDB with Zn(0) in aqueous solution, as well as during biotic transformation by *Sulfurospirillum multivorans*. A stepwise nucleophilic substitution may take place in aqueous alkaline solution and also occurs during biotic transformation by *Ancylobacter aquaticus* [24]. The two pathways involve different bond-cleavage mechanisms. Dibromoelimination is assumed to result in simultaneous cleavage of two C-Br bonds, while S_N2 reaction follows a stepwise cleavage of one C-Br bond [5,24].

92

2.2. Pathway-specific reaction rates and isotope fractionation

In order to simulate carbon and bromine isotopic evolution of EDB via different reactions, we track dual element isotopologues. The relative abundances of such isotopologues can be computed considering the occurrence of both stable carbon and bromine isotopes:

$$A_j = \binom{2}{a} \cdot X^a \cdot (1-X)^{2-a} \cdot \binom{2}{b} \cdot Y^b \cdot (1-Y)^{2-b} \quad (1)$$

where A is the relative abundance of the j^{th} EDB isotopologue containing a ^{13}C out of a total of two carbon atoms and b ^{81}Br out of a total of two bromine atoms. X and Y are the abundance of heavy carbon and bromine isotopes, respectively.

Position specific fractionation factors for the j^{th} EDB isotopologue can be calculated according to the corresponding apparent kinetic isotope effect (AKIE) derived from the observed bulk enrichment factors:

$$\alpha_{rp,C} = AKIE_C^{-1} \approx 1 + \frac{2}{z_C} \cdot \varepsilon_C \quad (2)$$

$$\alpha_{rp,Br} = AKIE_{Br}^{-1} \approx 1 + \frac{2}{z_{Br}} \cdot \varepsilon_{Br} \quad (3)$$

where α_{rp} is the fractionating factor at reactive position, ε is bulk enrichment factor, and z is the number of carbon or bromine atoms at reactive positions. In this work we calculated α_{rp} based on the AKIE values reported in Kuntze et al. (2016); however, α_{rp} could be also derived by fitting the proposed model to the raw isotope data.

We track the concentration change of each isotopologue considering a specific kinetic rate law. To illustrate the approach, a first-order kinetic formulation is considered in the following equations; however, as discussed for the application examples in Section 3, any degradation rate can be implemented, including Michaelis-Menten kinetics. Since different reaction mechanisms of EDB

involve carbon and bromine atoms located at different isotopically-sensitive positions, the reaction rates have to take into account all the fractionating atoms. Concerning the dibromoelimination reaction, the two C-Br bonds are cleaved simultaneously, and thus the reaction rate for a specific carbon-bromine isotopologue is given as:

$$r_j = k \cdot C_j \cdot (\alpha_{rp,C})^a \cdot (\alpha_{rp,Br})^b \quad (4)$$

where r_j is the reaction rate for the j^{th} isotopologue, k is the first-order reaction rate constant, C_j is the concentration of the j^{th} isotopologue, α_{rp} is the fractionation factor as defined in Eqs. (2) and (3).

Considering S_N2 reaction of EDB, such reaction pathway involves the cleavage of one single C-Br bond. In this case the reaction rate of EDB depends on the isotopic composition of the C-Br bond that is cleaved, and thus the reaction rate of the individual isotopologues is defined in a bond-specific manner as previously proposed for the carbon-chlorine isotope modelling of chlorinated ethenes [30]. Due to the fact that the two C-Br bonds of EDB are chemically equivalent for S_N2 reaction, the approach is based on isotopologues without the need of specifying individual isotopomers. Thus, the reaction rate, r_j , for a given j^{th} EDB isotopologue is expressed as the sum of the following bond-specific reaction rates:

$$r_{j,^{12}C-^{79}Br} = k \cdot C_j \cdot \frac{(2 - n_{rp,^{13}C})}{2} \cdot \frac{(2 - n_{rp,^{81}Br})}{2} \quad (5)$$

$$r_{j,^{13}C-^{79}Br} = k \cdot C_j \cdot \alpha_{rp,C} \cdot \frac{n_{rp,^{13}C}}{2} \cdot \frac{(2 - n_{rp,^{81}Br})}{2} \quad (6)$$

$$r_{j,^{12}C-^{81}Br} = k \cdot C_j \cdot \alpha_{rp,Br} \cdot \frac{(2 - n_{rp,^{13}C})}{2} \cdot \frac{n_{rp,^{81}Br}}{2} \quad (7)$$

$$r_{j,^{13}C-^{81}Br} = k \cdot C_j \cdot \alpha_{rp,C} \cdot \alpha_{rp,Br} \cdot \frac{n_{rp,^{13}C}}{2} \cdot \frac{n_{rp,^{81}Br}}{2} \quad (8)$$

$$r_j = \sum_{i=1}^N r_{j,(C-Br)_i} \quad (9)$$

125 where k is the first-order rate constant, C_j is the concentration of the j^{th} isotopologue, and n_{rp}
 126 represents the total number of reactive carbon or bromine atoms within the isotopologue, i indicates
 127 the C-Br bond cleaved during the reaction and N is the total number of C-Br bonds that can be
 128 cleaved for the j^{th} EDB isotopologue. Note that an overall rate for all isotopologues can be
 129 computed from the rate of each isotopologue as $\sum_{i=1}^m r_j$, where m is the total number of
 130 isotopologues. The concentration change of the j^{th} isotopologue of EDB is described as:

$$\frac{dC_j}{dt} = -r_j \quad (10)$$

131 The total concentration of EDB can be obtained by summing the concentrations of each
 132 isotopologue:

$$C_{tot} = \sum_{j=1}^m C_j \quad (11)$$

133

134 where C_{tot} is the total concentration of EDB, C_j is the concentration of the j^{th} isotopologue and m is
 135 the total number of EDB isotopologues.

136 The concentration of each isotopologue is used to calculate stable carbon and bromine isotope ratios
 137 by considering the total number of heavy and light isotopes [14] and are expressed as:

$$R_C = \frac{Tot(^{13}C)}{Tot(^{12}C)} = \frac{\sum_{j=1}^m a \cdot C_j}{\sum_{j=1}^m (2-a) \cdot C_j} \quad (12)$$

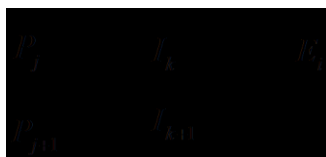
$$R_{Br} = \frac{Tot(^{81}Br)}{Tot(^{79}Br)} = \frac{\sum_{j=1}^m b \cdot C_j}{\sum_{j=1}^m (2-b) \cdot C_j} \quad (13)$$

138 where R_C and R_{Br} are the carbon and bromine isotope ratios of EDB, C_j is the concentration of the j^{th}
 139 isotopologue, m is the total number of EDB isotopologues as defined in Eq (11), a and b are the
 140 number of heavy carbon and heavy bromine isotopes, as defined in Eq (1).

141 2.3. Complex Reaction Pathways

142 In the previous section we illustrated the modelling for single step reactions. However, the model
 143 can be applied also when degradation occurs through more complex reaction pathways involving
 144 sequential and parallel reactions. In this cases, if one aims at describing the formation and
 145 consumption of intermediates and products and the evolution of their dual-element isotopic
 146 composition, it is necessary to take into account that a given intermediate (or product) can be
 147 formed by two distinct isotopologues of the parent compound (or intermediate).

148 Sequential multistep reactions. We consider EDB degradation through sequential multistep
 149 reactions, specifically, through a reaction pathway involving two S_N2 type reactions. As parent
 150 compound (P) the two different EDB isotopologues considered are: the j^{th} isotopologue and the
 151 $(j+1)^{th}$ isotopologue. The latter contains one more ^{81}Br isotope in the molecule compared to the j^{th}
 152 isotopologue. The parent compound (P) is sequentially degraded into the k^{th} and $(k+1)^{th}$
 153 isotopologues of the intermediate (I), and finally into the i^{th} isotopologue of the end product (E),
 154 which is completely debrominated. The two-step reaction can be illustrated as:



155 (14)

156 Note that the different letters used as subscripts indicate that the different compounds may have a
 157 different number of isotopologues.

158 The concentration of the isotopologues of the parent compound (P), the intermediate (I) and the end
 159 product (E) are described:

$$\frac{dP_j}{dt} = -r_{1,j} \quad (15)$$

$$\frac{dI_k}{dt} = +r_{1,j} + r_{1,j+1} - r_{2,k} \quad (16)$$

$$\frac{dE_i}{dt} = +r_{2,k} + r_{2,k+1} \quad (17)$$

160 where $r_{1,j}$, $r_{1,j+1}$, $r_{2,k}$ and $r_{2,k+1}$ are the isotopologue-specific reaction rates for the parent compound
 161 and for the intermediate, respectively. The kinetic formulation for such reaction rates $r_{1,j}$ and $r_{1,j+1}$
 162 (parent compound), as well as $r_{2,k}$ and $r_{2,k+1}$ (intermediate) are based on Eqs. 5-9. The carbon and
 163 bromine isotope ratios for the parent compound, intermediate and end product can be calculated
 164 according to Eqs. 12-13.

165 Parallel reactions. Competition between different reaction pathways of EDB degradation has been
 166 observed in several experimental studies [5,24]. We consider the case of EDB transformation
 167 through two competing reaction pathways that yield two different products:



169 The concentration of the j^{th} isotopologues of the parent compound (P_j) and the k^{th} and i^{th} of the two
 170 end products ($E_{A,k}$ and $E_{B,i}$) are given as:

$$\frac{dP_j}{dt} = -r_{A,j} - r_{B,j} \quad (19)$$

$$\frac{dE_{A,k}}{dt} = +r_{A,j} + r_{A,j+1} \quad (20)$$

$$\frac{dE_{B,i}}{dt} = +r_{B,j} + r_{B,j+1} \quad (21)$$

171 where $r_{A,j}$, $r_{A,j+1}$, $r_{B,j}$ and $r_{B,j+1}$ are the reaction rates for the individual reaction pathway of the j^{th}
 172 and $(j+1)^{\text{th}}$ isotopologue of the parent compound (P).

173 **2.4. Model implementation**

174 The governing equations describing the simultaneous evolution of the concentrations, as well as the
 175 carbon and bromine isotope ratios are implemented in MATLAB[®]. The system of ordinary
 176 differential equations is solved numerically using the function *ode15s*. The experimental data and
 177 the key isotope fractionation parameters are taken from the experimental work of Kuntze et al.
 178 (2016); the latter are summarized in Table 1. The simulation was run for a time covering the
 179 duration of the experiments (i.e., 4 hours for the two cases of dibromoelimination by both Zn(0) and
 180 *S. multivorans*, 350 hours for abiotic degradation in alkaline solution and 8 hours in the case of
 181 biotic degradation by *A. aquaticus*). The EDB concentration data were used to determine the kinetic
 182 parameters of the degradation rates. First-order and Michaelis-Menten kinetics were considered for
 183 the abiotic and biotic reaction pathways, respectively. A fitting procedure, minimizing the sum of
 184 normalized squared errors based on the function *lsqnonlin*, was used to obtain the values of the
 185 kinetic parameters. As illustrated above, the proposed approach tracks the dual-element EDB
 186 isotopologues. Nine EDB isotopologues were considered in the simulations by taking into account
 187 all possible combinations of carbon and bromine isotopes. The abundances of these isotopologues
 188 were determined based on Eq. 1.

189 **[insert Table 1 here]**

190

191 3. Results and discussion

192 3.1. Chemical and biotic dibromoelimination reactions

193 The dual carbon and bromine isotope approach has been used to investigate EDB degradation by
194 dibromoelimination reactions [24]. To reproduce the experimental data observed during
195 dibromoelimination reactions, we simulated carbon and bromine isotopic evolution according to the
196 hypothesized two-electron transfer dibromoelimination mechanism. The simulation results (solid
197 lines in Fig. 1) are shown together with the reported experimental data (symbols in Fig. 1). A first-
198 order kinetic ($k=0.9\text{ h}^{-1}$) is used to describe the concentration variation of EDB during
199 dibromoelimination by Zn(0) (Fig. 1a), where the concentration decreases down to 4.3% of the
200 initial concentration value. The model also accurately predicts the carbon and bromine isotope
201 fractionation (Fig. 1b), which are simulated based on the experimentally evaluated *AKIE* values
202 ($AKIE_C=1.0223$, $AKIE_{Br}=1.0042$) [24]. The results show different extents of carbon and bromine
203 fractionation, with $\delta^{13}\text{C}$ values changing from -26.3‰ to -3.8‰ and $\delta^{81}\text{Br}$ varying from 0.5‰ to
204 5.4‰. For biotic dibromoelimination, a Michaelis-Menten kinetics, with maximum degradation rate
205 $k_{max}=0.2289\text{ mmol}\cdot\text{L}^{-1}\cdot\text{h}^{-1}$ and half-saturation constant $K_s=0.0166\text{ mmol}\cdot\text{L}^{-1}$, is used in our model to
206 reproduce the observed concentration data during biotic dibromoelimination by *S. multivorans* (Fig.
207 1c). The carbon and bromine *AKIE* values of 1.0107 and 1.0046 are used in the model to describe
208 carbon and bromine isotope effects. The fractionation was introduced in the maximum degradation
209 rate and led to an increase of 12.7‰ for ^{13}C and of 6.2‰ for ^{81}Br isotopes during degradation of
210 about 95% of the initial EDB concentration.

211 [insert Figure 1 here]

212 Linear dual carbon-bromine isotopic trends with different slopes are obtained for chemical (slope of
213 5.3) and biotic (slope of 2.4) dibromoelimination reactions and the model accurately captures the
214 two different dual-isotope trends. The excellent agreement between experimental and modelling

215 results demonstrates the capability of the proposed mechanistic model to simultaneously capture the
216 evolution of both concentration and carbon-bromine stable isotopes.

217 **3.2. Chemical and biotic nucleophilic substitution (S_N2) reactions**

218 Nucleophilic substitution (S_N2) reaction is another important degradation mechanism for EDB. A
219 stepwise scenario is followed by both biotic and chemical S_N2 reactions, where the cleavage of one
220 carbon-bromine bond of EDB is hypothesized as the isotopically sensitive step. We provide a
221 model-based interpretation of the experimental data provided in the study of Kuntze et al. [24], who
222 observed carbon and bromine isotope fractionation of EDB during chemical degradation in aqueous
223 alkaline solution as well as during biotic S_N2 reaction by *Ancylobacter aquaticus*.

224 **[insert Figure 2 here]**

225 We use a first-order kinetics ($k=0.0125\text{ h}^{-1}$) to describe the concentration change during the
226 chemical S_N2 reaction (solid line in Fig. 2a). The corresponding carbon isotope ratio varies from -
227 11.6‰ to 93.8‰, and the bromine isotope fractionation occurs in a range between 0.4‰ and 4.3‰.
228 The biotic S_N2 reaction of EDB is described by a Michaelis-Menten kinetics with maximum
229 degradation rate ($k_{max}=0.4329\text{ mmol}\cdot\text{L}^{-1}\cdot\text{h}^{-1}$) and half-saturation constant ($K_s=0.0288\text{ mmol}\cdot\text{L}^{-1}$)
230 evaluated based on the observed concentration data (Fig. 2c). The simulation of carbon and bromine
231 isotope signals is based on the reported $AKIE$ values ($AKIE_C=1.062$ and $AKIE_{Br}=1.002$ for the
232 chemical S_N2 reaction; $AKIE_C=1.014$ and $AKIE_{Br}=1.0012$ for the biotic S_N2 reaction). The
233 simulations of the biotic and chemical S_N2 transformations of EDB were able to capture the
234 different fractionation of the two reaction pathways observed in the experiments. Specifically, the
235 biotic transformation resulted in a smaller extent of both carbon and bromine isotope fractionation
236 (17.9‰ for $\delta^{13}\text{C}$ and 1.8‰ for $\delta^{81}\text{Br}$) whereas the chemical S_N2 reaction resulted in stronger
237 fractionation (105.4‰ for $\delta^{13}\text{C}$ and 3.9‰ for $\delta^{81}\text{Br}$).

238

239 Fig. 3 summarizes the dual element isotope plots for the four cases of chemical and biotic EDB
240 degradation through dibromoelimination and S_N2 type nucleophilic substitution. The four different
241 reactions are adequately characterized in the dual carbon-bromine isotope plot. In all the cases the
242 simulation outcomes closely reproduce the experimental results. Note that these outcomes are no
243 linear fits of the experimental data, but represent mechanistic descriptions of EDB degradation
244 through different reaction pathways according to the approach outlined in Section 2. For all
245 considered cases of EDB degradation the normalized root mean squared error was calculated as a
246 quantitative measure of the goodness-of-fit. Such metric was computed for both carbon and
247 bromine isotope data and yielded values in a range of 0.036-0.158 for carbon and 0.068-0.16 for
248 bromine. The successful comparison of the simulation results with the experimental data highlights
249 the capability of the proposed approach to quantitatively describe different mechanisms of EDB
250 degradation.

251 **[insert Figure 3 here]**

252 ***3.3. Scenario modelling***

253 Based on the validated model presented above, we also investigated scenarios involving complex
254 EDB reaction pathways, such as sequential multistep reactions (Scenario 1 in Fig. 4) and parallel
255 reactions (Scenario 2 in Fig. 4). In the examples illustrated in the previous section and in most
256 experimental studies, the CSIA approach has been mainly focusing on the parent compound.
257 However, stable isotope analysis of reaction products can also be very informative about the
258 underlying reaction steps characterizing different reaction mechanisms [22,31]. To explore the
259 potential of carbon and bromine CSIA of EDB degradation products, we simulate the evolution of
260 the concentration and the isotopic signals of the parent compound, the intermediates and the end

261 products for the two proposed reaction scenarios illustrated in Fig. 4: 1) multistep S_N2 nucleophilic
262 substitution and 2) simultaneous occurrence of the S_N2 reaction and dehydrobromination.

263 **[insert Figure 4 here]**

264 The S_N2 reaction involves the stepwise cleavage of two C-Br bonds, kinetic isotope effects for C-Br
265 cleavage ($KIE_C=1.042$; $KIE_{Br}=1.002$) were calculated in the previous experimental study based on
266 the Streitwieser limit [24]. Since isotope fractionation of the intermediate has not been
267 experimentally determined (yet), the theoretical $KIEs$ values are used as model input parameters to
268 differentiate the reaction rates of the different carbon-bromine isotopologues of both parent and
269 intermediate compounds. The simulation results for sequential multistep EDB degradation
270 (Scenario 1) are shown in Fig. 5. The degradation of the parent compound EDB (blue solid line in
271 Fig. 5a) results in the formation of the intermediate, bromoethylene glycol (red dotted line, $k=0.5\text{ h}^{-1}$)
272 ¹), which is further transformed to ethylene glycol (green dash-dotted line, $k=2.5\text{ h}^{-1}$) that
273 accumulates as the end product. The temporal carbon and bromine isotope trends are reported in
274 Fig. 5b and 5c and show a linear increase of $\delta^{13}\text{C}$ and $\delta^{81}\text{Br}$ values for EDB. However, the
275 increasing trends of carbon and bromine isotope ratios become nonlinear for the intermediate,
276 bromoethylene glycol. This is due to the fact that bromoethylene glycol (red dotted line) further
277 degrades and preferentially transfers ^{12}C isotopes to the end product and meanwhile preferentially
278 releases ^{79}Br during its transformation. As a result, the $\delta^{13}\text{C}$ values of the end product, ethylene
279 glycol (green dash-dotted line), continuously increase and approach the original carbon isotope
280 signature of EDB. In the dual carbon-bromine isotope plot (Fig. 5d) EDB and bromoethylene glycol
281 have different trends. EDB shows a linear increase with a slope of 20.2, whereas a nonlinear curve,
282 with a slope varying from 11 to 21.5, describes the trend of bromoethylene glycol. This nonlinear
283 behaviour is due to the simultaneous formation and consumption of bromoethylene glycol, which
284 occur at different rates and involve different extents of carbon and bromine isotope fractionation

285 during the course of the degradation reaction. For multistep reactions with formation and further
286 degradation of intermediates, a mechanistic modelling approach is helpful since it allows the
287 simultaneous interpretation of isotope fractionation for both precursors and reaction products.

288 **[insert Figure 5 here]**

289 In Scenario 2, degradation of EDB in alkaline solution is considered. In this scenario two competing
290 reaction pathways, i.e., nucleophilic substitution (S_N2) and dehydrobromination, occur
291 simultaneously. Concerning dehydrobromination, this reaction pathway involves the simultaneous
292 cleavage of a carbon-bromine bond and a carbon-hydrogen bond. The theoretical carbon and
293 bromine isotopic effects during cleavage of C-H ($KIE_C=1.021$) and C-Br ($KIE_C=1.042$; $KIE_{Br}=1.002$)
294 bonds [24,36] are considered to calculate the fractionation factors at reactive positions used in the
295 isotopologue-specific rate expression (Eq. 4). We applied the model to simulate concentrations and
296 isotope ratios for such a parallel reaction system. We assume that the two reactions follow a first-
297 order kinetic with rate constants of 0.5 h^{-1} and 0.03 h^{-1} for S_N2 reaction and dehydrobromination,
298 respectively. These values were selected according to the relative contribution of 93% (sequential
299 S_N2 reaction) and 7% (dehydrobromination) observed in the experimental study of Kuntze et al.
300 [24]. The evolution of concentration, carbon and bromine isotopic signals is simultaneously
301 simulated for EDB, the intermediate and the end products. As shown in Fig. 6a, the two competing
302 degradation reactions cause a decrease of the EDB concentration (blue solid line). The intermediate,
303 bromoethylene glycol (red dotted line), is formed and further degrades into ethylene glycol (green
304 dash-dotted line) by nucleophilic substitution (S_N2). In parallel, dehydrobromination causes the
305 formation of vinyl bromide (black solid line). Fig. 6b illustrates the $\delta^{13}\text{C}$ trends for the species
306 involved in the two reaction pathways: the parent compound shows a linear behaviour, whereas the
307 intermediate and the end products show nonlinear curves with decreasing slope. Bromine stable
308 isotope ratios are shown in Fig. 6c. Stable bromine isotope fractionation occurs at different extents

for the two brominated degradation products: $\delta^{81}\text{Br}$ is enriched by 7.6‰ for bromoethylene glycol ($\text{S}_{\text{N}}2$ reaction) and by 1‰ for vinyl bromide (dehydrobromination), because the former is an intermediate which undergoes further debromination, whereas vinyl bromide represents a final product in this scenario. In the dual-isotope plot (Fig. 6d) a linear trend is obtained for the parent compound EDB (slope: 21.2), as well as for vinyl bromide from the dehydrobromination reaction (slope: 20.3). A nonlinear dual-isotope trend is obtained for the $\text{S}_{\text{N}}2$ reaction intermediate, bromoethylene glycol, with a slope varying from 11.1 to 22.9. The dual isotope trend of EDB (blue line in Fig. 6d) appears very similar with the one obtained during 100% $\text{S}_{\text{N}}2$ reaction (lower dashed line). This is due to the fact that, in the considered scenario, the $\text{S}_{\text{N}}2$ reaction is the dominant pathway (about 93% contribution) during EDB degradation in alkaline solution. The shaded grey area between the dotted lines indicates the possible range for the investigated scenario: from 100% contribution of dehydrobromination (upper bound) to 100% contribution of the $\text{S}_{\text{N}}2$ reaction (lower bound). The dual element isotope signatures of the reaction products from the different pathways have a distinct behaviour and are different from the trend of the parent compound. The simulation results indicate that in practice it might be difficult to accurately quantify the contribution of each concurrent reaction pathway exclusively based on the observed EDB carbon and bromine isotope data. However, these simulations also demonstrate that CSIA of reaction intermediates and end products can bring new possibilities to elucidate the underlying reaction steps and to accurately quantify the contributions of individual reaction pathways.

[insert Figure 6 here]

4. Conclusion

Dual carbon-bromine isotope investigation significantly improves the understanding of various reaction mechanisms of brominated organic compounds. Recent studies have focused on the

development of analytical techniques for bromine CSIA as well as experimental investigation of degradation mechanisms of different brominated organic pollutants. In this study, we have proposed an integrated modelling approach allowing the simultaneous prediction of concentrations and dual-element isotope ratios. Our investigation focused on carbon and bromine isotope fractionation during 1,2-dibromoethane (EDB, ethylene dibromide) transformation through different reaction pathways. The proposed modelling approach tracks dual-element isotopologues. The method allowed us reproducing the carbon and bromine isotopic signal observed in experimental studies of different chemical and biotic EDB reaction pathways. The approach is based on bond-specific reaction rates and can be readily extended to cases in which different contaminants and/or reaction pathways will require tracking also isotopomers (i.e., molecules with the same number of each isotopic atom but differing in their position). Furthermore, we exemplified the model capabilities with two scenarios involving complex reaction systems with sequential and parallel reactions, respectively. In the considered case of multistep nucleophilic substitution (S_N2) reaction, concentration and isotopic ratios of the parent compound, the intermediate and the end product were predicted based on the validated model. Different carbon and bromine isotopic behaviours of the parent compound and intermediate were obtained. In the scenario modelling of EDB degradation via two concurrent reactions, our simulation results showed that stable isotope analysis of the reaction products is beneficial, since it allows quantifying further degradation of the intermediate product in multistep reactions, as well as providing a more accurate evaluation of the individual contributions of different concurrent pathways to the overall reaction. This is particularly beneficial when one of the reaction pathways is dominant and, therefore the sole analysis of the dual isotope trend of the parent compound would not be conclusive in identifying which degradation reactions are responsible for the contaminant degradation. The proposed model was applied to the specific case of EDB degradation, however it provides a framework that can be extended to other

356 brominated compounds that may undergo degradation through different reaction pathways. The
357 first-principle based formulation of the approach will also facilitate future model-based applications
358 in complex environmental systems, in which both transformation and mass transfer processes may
359 affect the observed isotope signals.

360 **Acknowledgements**

- 361 • The authors thank Dr. Kevin Kuntze for providing the experimental data that were used to test
362 the modelling approach and two anonymous reviewers for their comments that helped
363 improving the manuscript.
- 364 • B.J. and M.R. acknowledge the support of the Deutsche Forschungsgemeinschaft (grant
365 RO4169/2-1) and of the Sino-Danish Center (SDC).
- 366 • B.J. acknowledges the support of CAS Pioneer Hundred Talents Program
367
- 368 • I.N. acknowledges the support of the Deutsche Forschungsgemeinschaft (grant FOR1530
369 NI1329/1-2)

370

371

372

373

374

375

376

377

378

379

380

381

382 **Table 1.** Reaction mechanisms, bulk enrichment factors (ϵ_{bulk}) and fractionation factors at reactive position
383 (α_{rp}) for the different EDB degradation reactions.

Reaction	Mechanism	ϵ_{bulk}		α_{rp}	
		C	Br	C	Br
Zn (0)	dibromoelimination	-10.9±1.1	-2.1±0.3	0.9891±0.0011	0.9979±0.0003
<i>S. multivorans</i>	dibromoelimination	-5.3±0.5	-2.3±0.2	0.9947±0.0005	0.9977±0.0002
Alkaline solution	abiotic S _N 2	-29.2±2.6	-1.0±0.1	0.9416±0.0052	0.9980±0.0002
<i>A. aquaticus</i>	biotic S _N 2	-6.9±0.4	-0.6±0.1	0.9862±0.0008	0.9988±0.0002

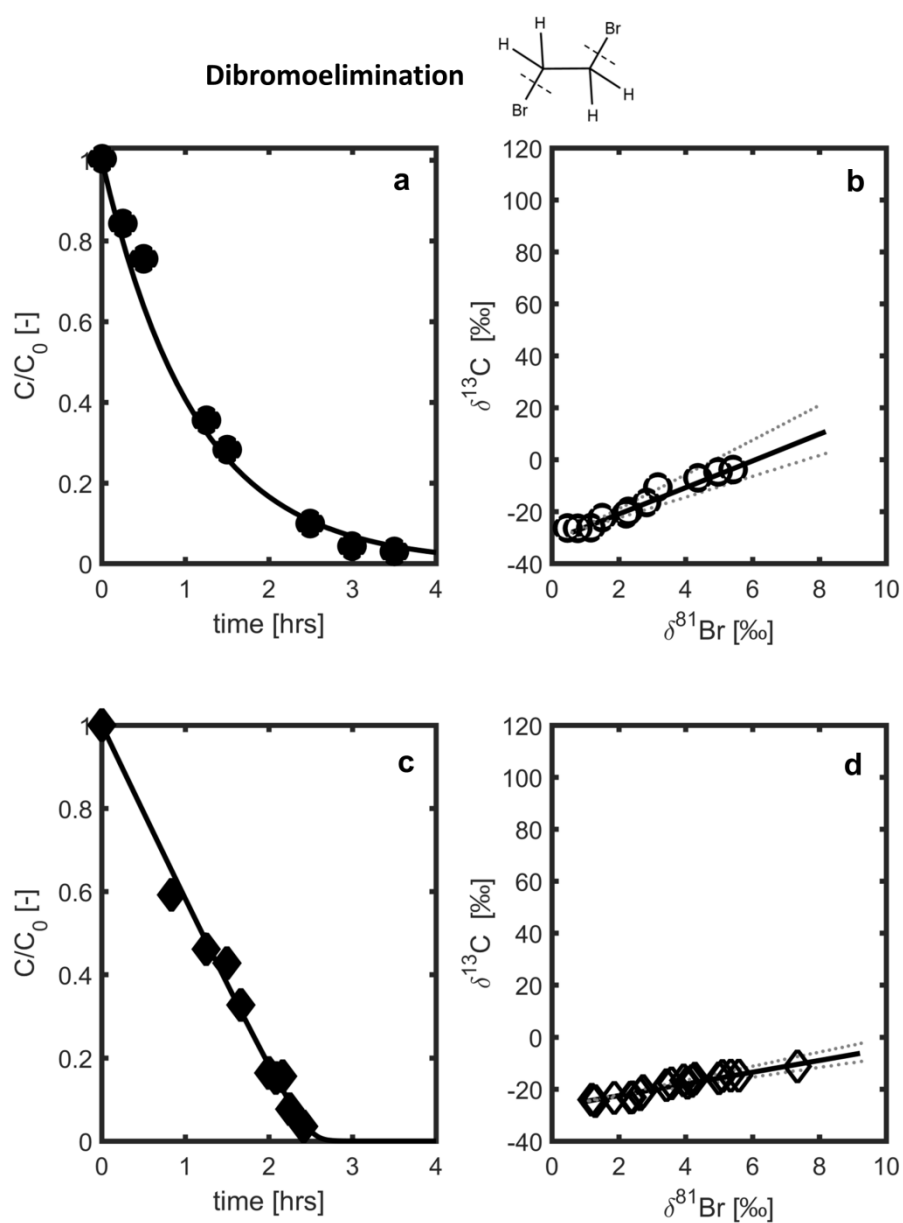
384

385

386

387

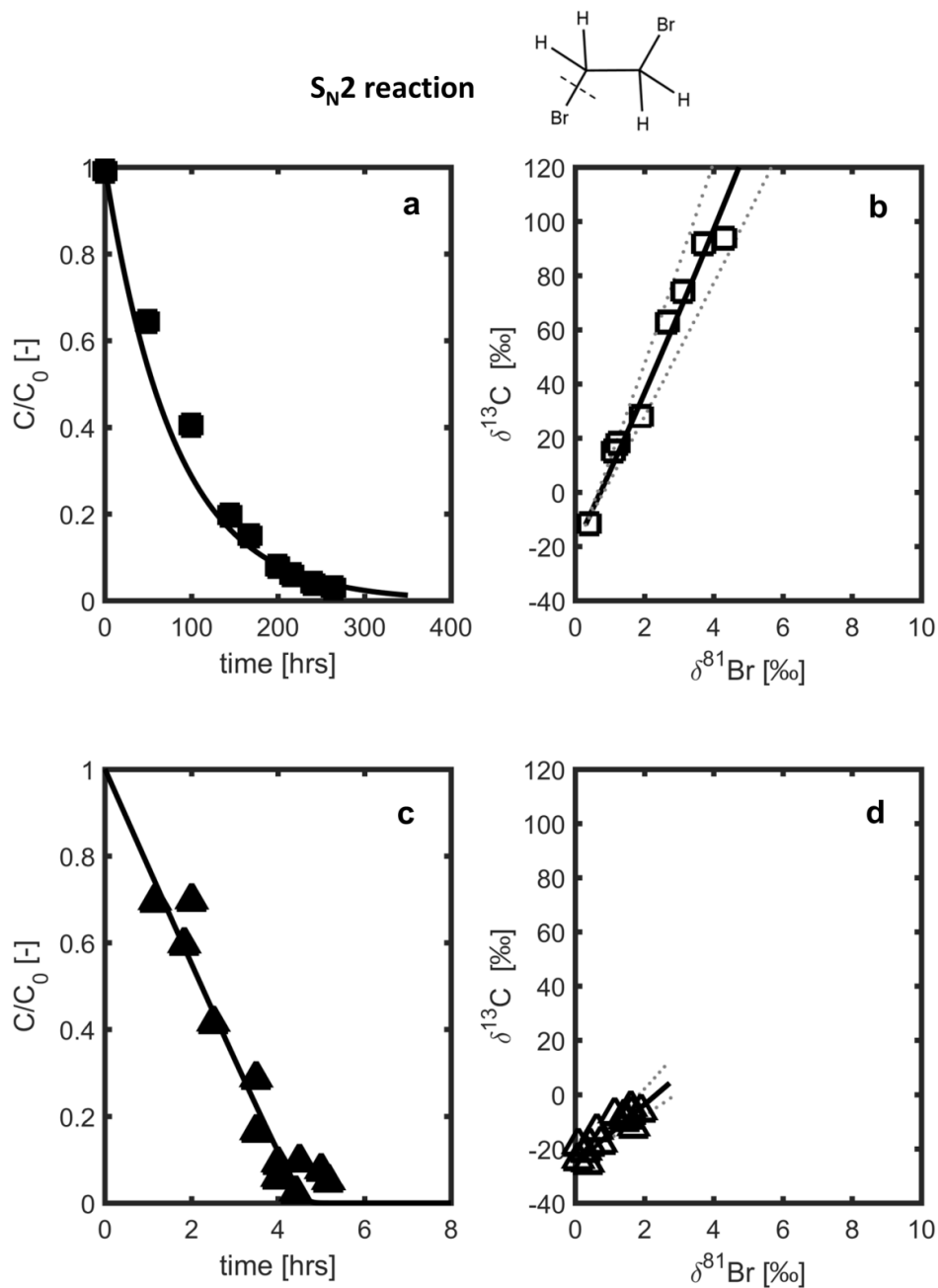
388



389

390 **Figure 1.** Concentration change and dual carbon-bromine isotope fractionation during dibromoelimination
 391 reaction by Zn(0) (Panels (a) and (b)) and biotic reaction with *S. multivorans* (Panels (c) and (d)). The
 392 symbols represent the experimental data reported in Kuntze et al. [24], and the solid lines are the simulation
 393 results.

394



395

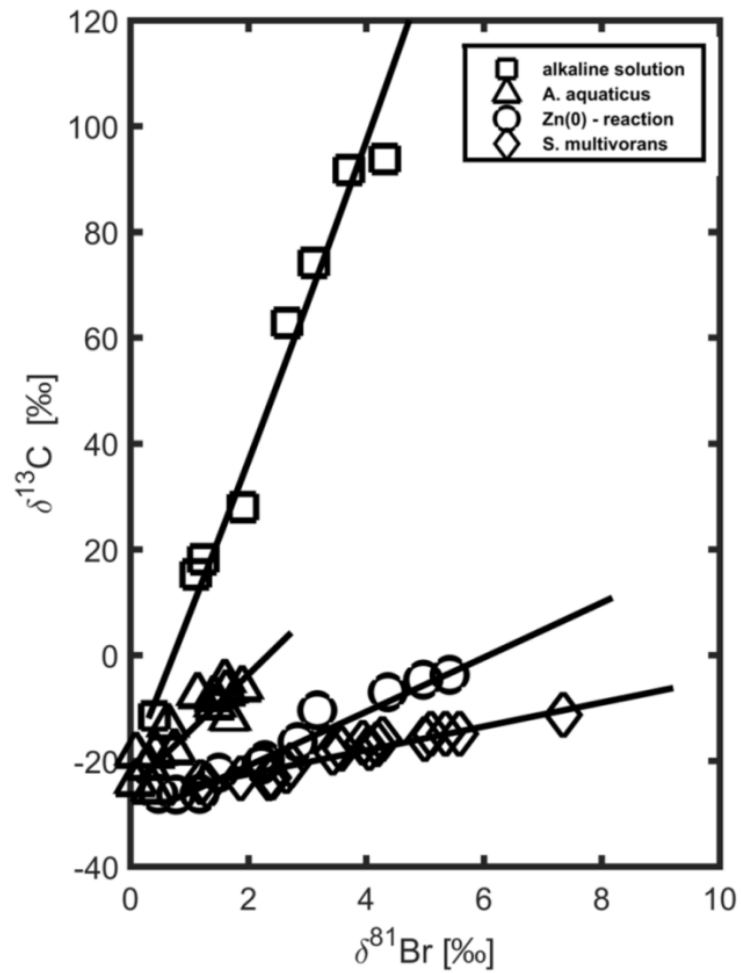
396 **Figure 2.** Carbon and bromine isotope fractionation during EDB chemical transformation in alkaline
 397 solution and biotic reaction by *Ancylobacter aquaticus*. Panel (a) and (c): the symbols represent the observed
 398 concentration profiles reported in Kuntze et al. [24], and the lines are the simulation results. Panel (b) and (d):
 399 the symbols are carbon-bromine isotopic data and the solid lines are the simulation results.

400

401

402

403



404

405 **Figure 3.** Carbon and bromine isotope fractionation for different EDB degradation reactions. The symbols
 406 represent the experimental data reported in Kuntze et al.[24], and the solid lines represent the results of the
 407 simulations corresponding to 99% degradation of the initial EDB concentration.

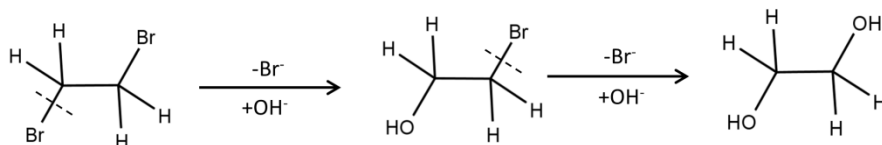
408

409

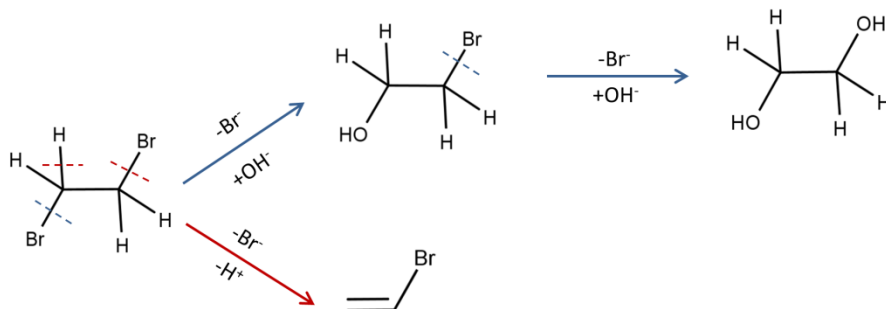
410

411

Scenario 1: Multistep reactions by nucleophilic substitution (S_N2)



Scenario 2: Parallel reactions in alkaline solution (nucleophilic substitution and dehydrobromination)



412

413 **Figure 4.** Schemes representing the sequential and parallel reaction pathways considered in the scenario
414 modelling.

415

416

417

418

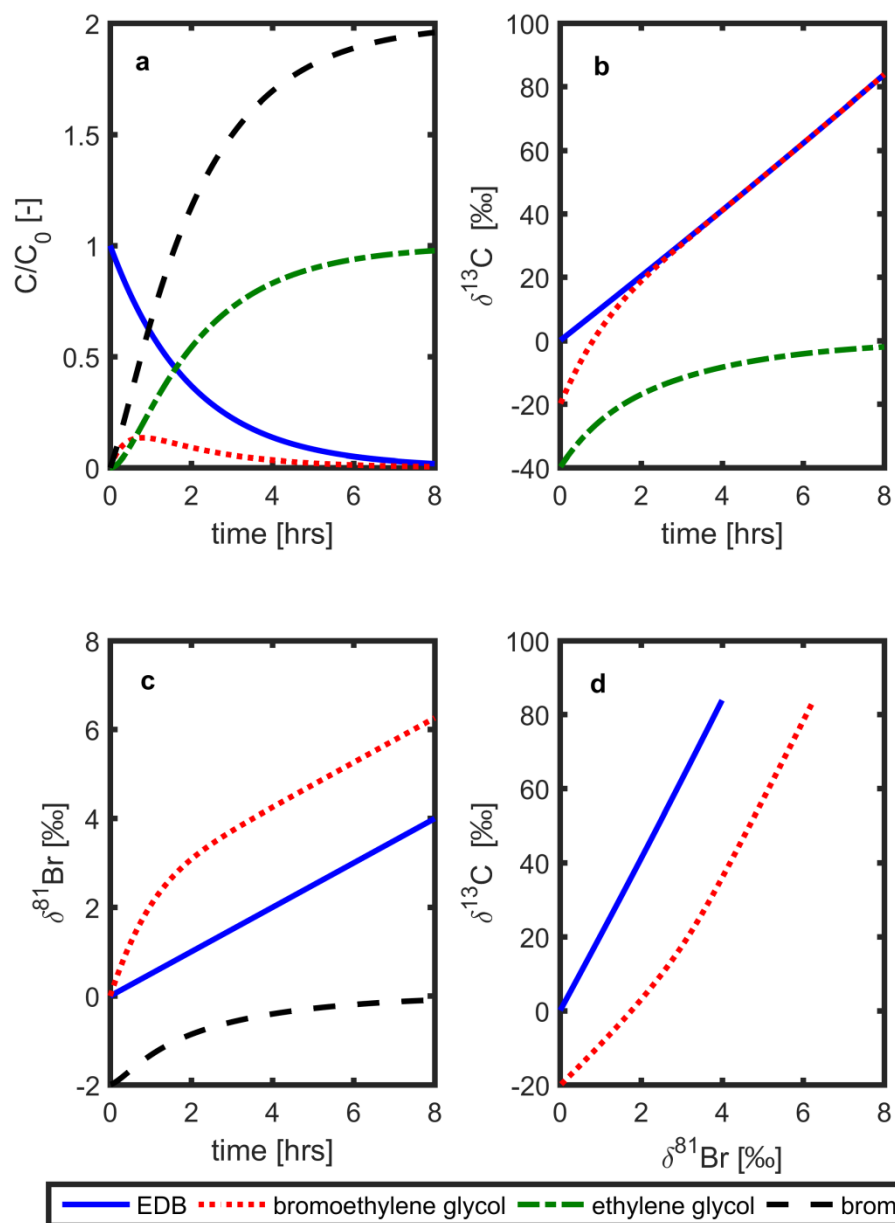
419

420

421

422

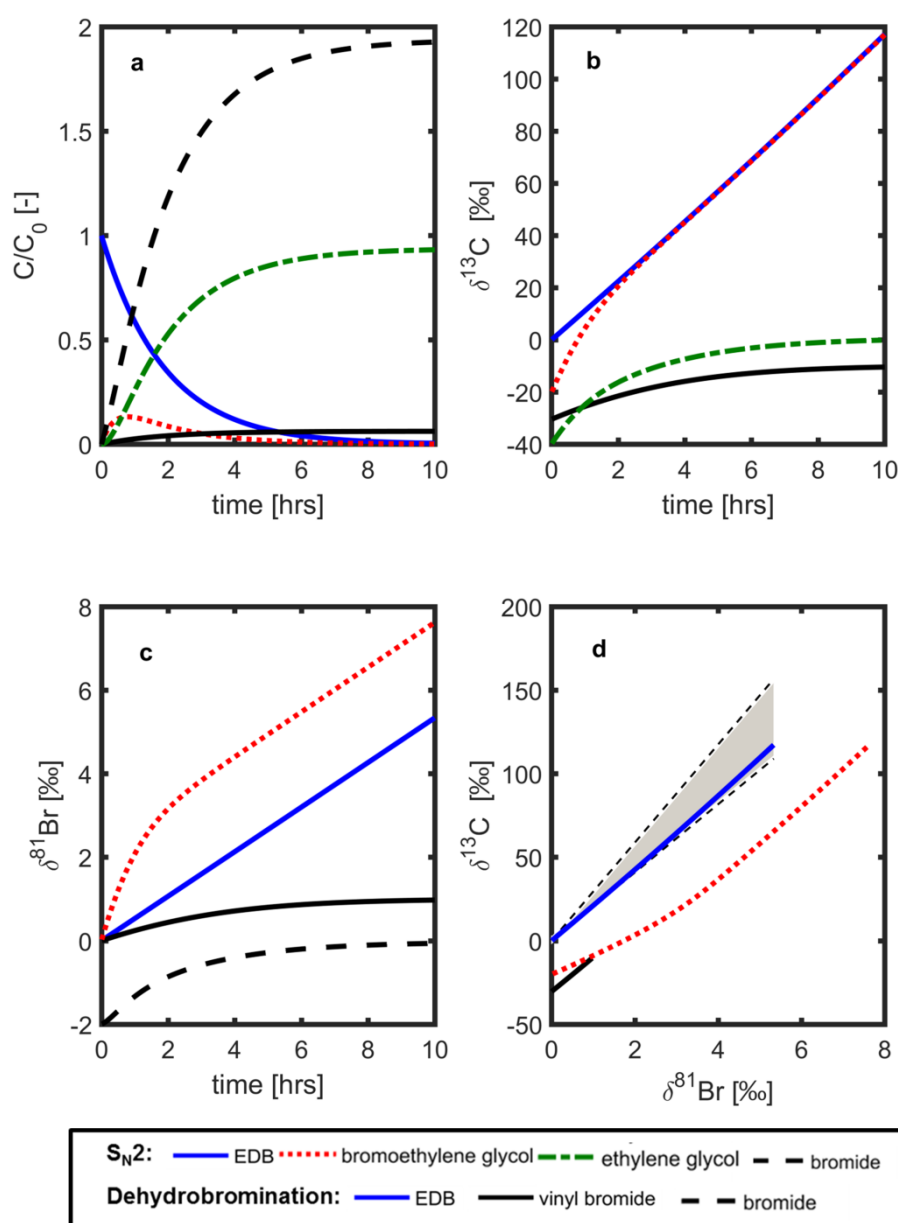
423



424

425 **Figure 5.** Concentration, carbon and bromine isotope fractionation of EDB, the intermediate (bromoethylene
 426 glycol), the end product (ethylene glycol) and bromide during multi-step nucleophilic substitution (Scenario
 427 1 in Fig. 4).

428



429

430 **Figure 6.** Concentration, carbon and bromine isotope fractionation of EDB during the two competing
 431 reaction pathways: nucleophilic substitution (S_N2) reaction and dehydrobromination (Scenario 2 in Fig. 4).
 432 The shaded area in Panel (d) indicates EDB dual-isotope trends corresponding to different contributions of
 433 each reaction pathway considered in Scenario 2. The dotted lines on the upper and lower bounds represent
 434 dual-isotope trends of EDB degradation when one reaction pathway occurs exclusively (i.e., 100%
 435 dehydrobromination and 100% S_N2 reaction, respectively).

436

437 **References**

- 438 [1] Falta RW, Bulsara N, Henderson JK, et al. Leaded-gasoline additives still contaminate groundwater.
439 *Environ. Sci. Technol.* 2005;39:379A–384A.
- 440 [2] Wilson, John T, Banks, Kenneth, Earle, Robert, He, Yongtian, Kuder, Tomasz, Adair C. Natural
441 attenuation of the lead scavengers 1,2-dibromoethane (EDB) and 1,2-dichloroethane (1,2-DCA) at
442 motor fuel release sites and implications for risk management. U.S. EPA. 2008.
- 443 [3] Yu R, Peethambaram HS, Falta RW, et al. Kinetics of 1,2-dichloroethane and 1,2-dibromoethane
444 biodegradation in anaerobic enrichment cultures. *Appl. Environ. Microbiol.* 2013;79:1359–1367.
- 445 [4] McKeever R, Sheppard D, Nüsslein K, et al. Biodegradation of ethylene dibromide (1,2-
446 dibromoethane [EDB]) in microcosms simulating in situ and biostimulated conditions. *J. Hazard.*
447 *Mater.* 2012;209–210:92–98.
- 448 [5] Kuder T, Wilson JT, Philp P, et al. Carbon isotope fractionation in reactions of 1,2-dibromoethane
449 with FeS and hydrogen sulfide. *Environ. Sci. Technol.* 2012;46:7495–7502.
- 450 [6] Bosma TNP, Middeldorp PJM, Schraa G., Zehender AJB. Mass Transfer Limitation of
451 Biotransformation: Quantifying Bioavailability. *Environ. Sci. Technol.* 1997;31:248–252.
- 452 [7] Rolle M, Kitanidis PK. Effects of compound-specific dilution on transient transport and solute
453 breakthrough: A pore-scale analysis. *Adv. Water Resour.* 2014;71:186–199.
- 454 [8] Schüth C, Taubald H, Bolaño N, et al. Carbon and hydrogen isotope effects during sorption of
455 organic contaminants on carbonaceous materials. *J. Contam. Hydrol.* 2003;64:269–281.
- 456 [9] Nijenhuis I, Richnow HH. Stable isotope fractionation concepts for characterizing biotransformation
457 of organohalides. *Curr. Opin. Biotechnol.* 2016;41:108–113.
- 458 [10] Elsner M, Imfeld G. Compound-specific isotope analysis (CSIA) of micropollutants in the
459 environment - current developments and future challenges. *Curr. Opin. Biotechnol.* 2016;41:60–72.
- 460 [11] Schmidt TC, Jochmann M a. Origin and Fate of Organic Compounds in Water: Characterization by
461 Compound-Specific Stable Isotope Analysis. *Annu. Rev. Anal. Chem.* 2012;5:133–155.
- 462 [12] Rosell M, Gonzalez-Olmos R, Rohwerder T, et al. Critical evaluation of the 2D-CSIA scheme for
463 distinguishing fuel oxygenate degradation reaction mechanisms. *Environ. Sci. Technol.*
464 2012;46:4757–4766.
- 465 [13] Sakaguchi-Söder K, Jager J, Grund H, et al. Monitoring and evaluation of dechlorination processes
466 using compound-specific chlorine isotope analysis. *Rapid Commun. Mass Spectrom.* 2007;21:3077–
467 3084.
- 468 [14] Jin B, Laskov C, Rolle M, et al. Chlorine Isotope Analysis of Organic Contaminants Using GC–qMS:
469 Method Optimization and Comparison of Different Evaluation Schemes. *Environ. Sci. Technol.*
470 2011;45:5279–5286.
- 471 [15] Gelman F, Halicz L. High precision determination of bromine isotope ratio by GC-MC-ICPMS. *Int. J.*
472 *Mass Spectrom.* 2010;289:167–169.
- 473 [16] Hitzfeld KL, Gehre M, Richnow HH. A novel online approach to the determination of isotopic ratios
474 for organically bound chlorine, bromine and sulphur. *Rapid Commun. Mass Spectrom.*
475 2011;25:3114–3122.

- 476 [17] Bernstein A, Shouakar-Stash O, Ebert K, et al. Compound-Specific Chlorine Isotope Analysis: A
477 Comparison of Gas Chromatography/Isotope Ratio Mass Spectrometry and Gas
478 Chromatography/Quadrupole Mass Spectrometry Methods in an Interlaboratory Study. *Anal. Chem.*
479 2011;83:7624–7634.
- 480 [18] Audí-Miró C, Cretnik S, Torrentó C, et al. C, Cl and H compound-specific isotope analysis to assess
481 natural versus Fe(0) barrier-induced degradation of chlorinated ethenes at a contaminated site. *J.*
482 *Hazard. Mater.* 2015;299:747–754.
- 483 [19] Nijenhuis I, Kuntze K. Anaerobic microbial dehalogenation of organohalides-state of the art and
484 remediation strategies. *Curr. Opin. Biotechnol.* 2016;38:33–38.
- 485 [20] Cretnik S, Thoreson K a., Bernstein A, et al. Reductive dechlorination of TCE by chemical model
486 systems in comparison to dehalogenating bacteria: Insights from dual element isotope analysis
487 ($^{13}\text{C}/^{12}\text{C}$, $^{37}\text{Cl}/^{35}\text{Cl}$). *Environ. Sci. Technol.* 2013;47:6855–6863.
- 488 [21] Bernstein A, Ronen Z, Levin E, et al. Kinetic bromine isotope effect: Example from the microbial
489 debromination of brominated phenols. *Anal. Bioanal. Chem.* 2013;405:2923–2929.
- 490 [22] Schmidt M, Lege S, Nijenhuis I. Comparison of 1,2-dichloroethane, dichloroethene and vinyl
491 chloride carbon stable isotope fractionation during dechlorination by two Dehalococcoides strains.
492 *Water Res.* 2014;52:146–154.
- 493 [23] Palau J, Cretnik S, Shouakar-Stash O, et al. C and Cl Isotope Fractionation of 1,2-Dichloroethane
494 Displays Unique $\delta^{13}\text{C}/\delta^{37}\text{Cl}$ Patterns for Pathway Identification and Reveals Surprising C–Cl
495 Bond Involvement in Microbial Oxidation. *Environ. Sci. Technol.* 2014;48:9430–9437.
- 496 [24] Kuntze K, Kozell A, Richnow HH, et al. Dual Carbon–Bromine Stable Isotope Analysis Allows
497 Distinguishing Transformation Pathways of Ethylene Dibromide. *Environ. Sci. Technol.*
498 2016;50:9855–9863.
- 499 [25] Eckert D, Rolle M, Cirpka O a. Numerical simulation of isotope fractionation in steady-state
500 bioreactive transport controlled by transverse mixing. *J. Contam. Hydrol.* 2012;140–141:95–106.
- 501 [26] Jin B, Rolle M, Li T, et al. Diffusive fractionation of BTEX and chlorinated ethenes in aqueous
502 solution: Quantification of spatial isotope gradients. *Environ. Sci. Technol.* 2014;48:6141–6150.
- 503 [27] Van Breukelen BM, Rolle M. Transverse hydrodynamic dispersion effects on isotope signals in
504 groundwater chlorinated solvents plumes. *Environ. Sci. Technol.* 2012;46:7700–7708.
- 505 [28] Hofstetter TB, Reddy CM, Heraty LJ, et al. Carbon and chlorine isotope effects during abiotic
506 reductive dechlorination of polychlorinated ethanes. *Environ. Sci. Technol.* 2007;41:4662–4668.
- 507 [29] Hunkeler D, Van Breukelen BM, Elsner M. Modeling chlorine isotope trends during sequential
508 transformation of chlorinated ethenes. *Environ. Sci. Technol.* 2009;43:6750–6756.
- 509 [30] Jin B, Haderlein SB, Rolle M. Integrated carbon and chlorine isotope modeling: Applications to
510 chlorinated aliphatic hydrocarbons dechlorination. *Environ. Sci. Technol.* 2013;47:1443–1451.
- 511 [31] Kuder T, Van Breukelen BM, Vanderford M, et al. 3D-CSIA: Carbon, chlorine, and hydrogen isotope
512 fractionation in transformation of TCE to ethene by a dehalococcoides culture. *Environ. Sci. Technol.*
513 2013;47:9668–9677.
- 514 [32] Thullner M, Centler F, Richnow H-H, et al. Quantification of organic pollutant degradation in
515 contaminated aquifers using compound specific stable isotope analysis – Review of recent
516 developments. *Org. Geochem.* 2012;42:1440–1460.

- 517 [33] Jin B, Rolle M. Mechanistic approach to multi-element isotope modeling of organic contaminant
518 degradation. *Chemosphere*. 2014;95:131–139.
- 519 [34] Jin B, Rolle M. Position-specific isotope modeling of organic micropollutants transformation through
520 different reaction pathways. *Environ. Pollut.* 2016;210:94–103.
- 521 [35] Jin B, Rolle M. Joint interpretation of enantiomer and stable isotope fractionation for chiral pesticides
522 degradation. *Water Res.* 2016;105:178–186.
- 523 [36] Elsner M, Zwank L, Hunkeler D, et al. A new concept linking observable stable isotope fractionation
524 to transformation pathways of organic pollutants. *Environ. Sci. Technol.* 2005;39:6896–6916.
- 525
- 526